

Microwave Studies for Dynamic Nuclear Polarization With COMSOL Multiphysics

M. Worcester, D. Keller

ABSTRACT: COMSOL Multiphysics 5.3 was used to simulate various microwave conditions to better understand how to optimize transfer and geometry for used with the Jefferson Lab Hall B dual polarization target. These studies are meant to study both the less understood behavior of microwaves in a cryostat but also the validity of the COMSOL suite for this particular application. We use our simulations of microwaves at 140 GHz to showed the behavior of guided waves both in the presence and absence of boundary conditions. Variation of parameters of waveguides, horns, and cavities revealed resonance conditions that can be used to optimized cryostat design. Geometries several orders of magnitude larger than the wavelength could not be effectively modeled in 3D, but were modeled using a 2D axially symmetric analog.

Contents

red1. Introduction	1
red2. Dual Helicity Nose	2
red2.1 Initial Studies	2
red2.2 The Model	3
red3. Initial Simulations	4
red3.1 Starting Metrics	6
red3.2 Simplified Geometry	6
red3.3 Further Limitations	10
red4. Empirical Studies	10
red4.1 Material Studies	10
red4.2 Microwave Cavity Studies	13
red4.3 2D Axisymmetry and Microwave Heating	14
red4.4 Horn Studies	18
red5. Waveguide Studies	24
red5.1 Slotted Waveguide	26
red6. Conclusion	29

1. Introduction

The longitudinally polarized target program in Hall-B seeks to incorporate a target system which can polarize positively and negatively using two separate polarized target cells in the beam-line simultaneously. The draw-back of the traditional single cell target system is that significant time dependent errors acquired during data collection at two separate times for each helicity can lead to false asymmetries. This type of uncertainty limits the scale that can be probed for small asymmetries. Significant reduction of this type of uncertainty can be achieved by having two targets polarized in opposite directions in the beam-line to collect data in both helicity states at the same time. One of the critical challenges which still must be addressed is how best to implement DNP irradiation on two cells at the same time with one source so that the microwave power each cell receives is similar and maximized. This will allow both cells to be ready for beam on a similar time scale as well as reach and maintain an optimal polarization level through the course of the experiment. We give a general overview of our various studies to try to acquire some broader characteristics that may be helpful in the near future.

COMSOL Multiphysics has been used to simulate the nose cavity which can later guide prototyping and future work on a physical model. COMSOL is a software suite that finite elements to approximate the physical systems and then solves each element individually for a desired timescale or frequency domain. While it is a sophisticated solver for frequency-independent Maxwell systems, the complexity of wave mechanics and electrodynamics make the effectiveness of solving stationary 3D systems at radio frequency of interest (140 GHz) very difficult. There are some techniques we explore and discuss that give reasonably accurate information for a particular set of assumptions.

The finite element method approximates the solution within each element, using some elementary shape function that can be constant, linear, or of higher order. Depending on the element order in the model, a finer or coarser mesh is required to resolve the solution. In general, there are three problem-dependent factors that determine the necessary mesh resolution. The first is the variation in the solution due to geometrical factors. The mesh generator automatically generates a finer mesh where there is a lot of fine geometrical details. Try to remove such details if they do not influence the solution, because they produce a lot of unnecessary mesh elements. The second is the skin effect or the field variation due to losses. It is easy to estimate the skin depth from the conductivity, permeability, and frequency. At least two linear elements per skin depth are required to capture the variation of the fields. If the skin depth is not studied or a very accurate measure of the dissipation loss profile is not needed, replace regions with a small skin depth with a boundary condition, thereby saving elements. If it is necessary to resolve the skin depth, the boundary layer meshing technique can be a convenient way to get a dense mesh near a boundary. The third and last factor is the wavelength. To resolve a wave properly, it is necessary to use about 10 linear (or five 2nd order) elements per wavelength. Keep in mind that the wavelength depends on the local material properties.

This note starts with an introduction and overview of the process of testing some geometries of the target nose piece using the microwave module is given in Section 2. ...

2. Dual Helicity Nose

The goal of our study is to simulate various geometric configurations using COMSOL Multiphysics and determine the accuracy and overall effectiveness of the simulations to be used in the optimization of a cryostat shape for the purpose of a dual helicity target.

2.1 Initial Studies

When energy from electromagnetic fields is transformed into thermal energy, RF heating occurs which in a cryostat is usually not preferred. There are two different types of RF heating methods: induction and dielectric. Induction heating takes place in materials with a high electrical conductivity, such as copper or other metals. Eddy currents are induced by the alternating electromagnetic field and the resistive losses heat up the material. Dielectric heating, on the other hand, happens in nonconducting material, when it's subjected to a high-frequency electromagnetic field. The alternating electromagnetic field causes the dielectric molecules to flip back and forth and the material to heat up due to internal friction.

Microwave power distribution is crucial to target polarization and can be coupled into resonant cavities to maintain electromagnetic oscillations when there is resistive damping. The topic of power coupling to resonant cavities involves detailed application of microwave theory. For the most part if each target cell receives a healthy dose the cooling power of the fridge can take care of the rest, but still an understanding of basic power coupling processes may be of interest when trying to optimize for two different locations in the cryostat. Geometry optimization to our knowledge has never been studied in detail for DNP polarization.

The dispersion relationship relates frequency and wavenumber for a propagating wave. We also try to consider the implications of dispersion relationships for electromagnetic waves propagating in metal structures. The waveguide, horn and cavity and the propagation velocity for modulations of frequency or amplitude can have interplay which can also effect optimization. In most cases letting the microwave bounce around in the cryostat has always been a reasonable approach and has got the job done. Our preliminary simulations studies seem to indicate that there may be more efficient way to use the power provided by the microwave generator but that this is highly frequency and geometry dependent.

Another critical point in our initial investigation is that the use of this particular simulation platform to study real world configurations is computationally prohibitively. To get useful comparisons significant simplification and approximation are necessary. In this way we try to explore the best methods to use COMSOL to gain insight on the microwave system behavior that can to some extent be tested experimentally in hopes of establishing some fiducial procedures.

2.2 The Model

Our initial model was based off of a simple physical prototype we constructed using COMSOL primitives as a control and bench-marked for further prototyping Figure 1. The microwaves are guided into the cavity through the circular waveguide that enters through the top of the nose. The staggered wedge redirects them towards the area where the cups would be positioned. In the figure outer transparent and the Kel-F cups are removed. This model was studied using the RF Microwave module so that the relative intensity could be inferred. Using the open-ended geometry no clear advantage we established in using COMSOL as compared to using a simple line tracing method or calculating averaged trajectory. However for close or partially close geometry resonance condition arise that are difficult to predict. However the sensitivity of the resonant behavior to the geometry, frequency, and materials along with boundary conditions only emphasizes the need to have a reliable setup. The limitations in COMSOL 3D computations means that most of the time the resonant conditions is forming from the reduction of complexity and not really reflecting a physics situation.

From this basic premise different geometries were designed just to test the general practicality of the simulations. First the structure at the end of the waveguide was eliminated and the geometry of the cavity itself was used to guide the microwave. Different end-caps were tested, such as flat disks and smaller hemispheres. Staggered cavity walls and multiple positions of the incoming waveguide have also been studied, but all variations use an aluminum cavity with some type of circular waveguide and two cups.

Another challenging parameter to simulate was the absorption properties of the material in the cups. At resonance the target material is expected to behave more like an absorber. Obtaining

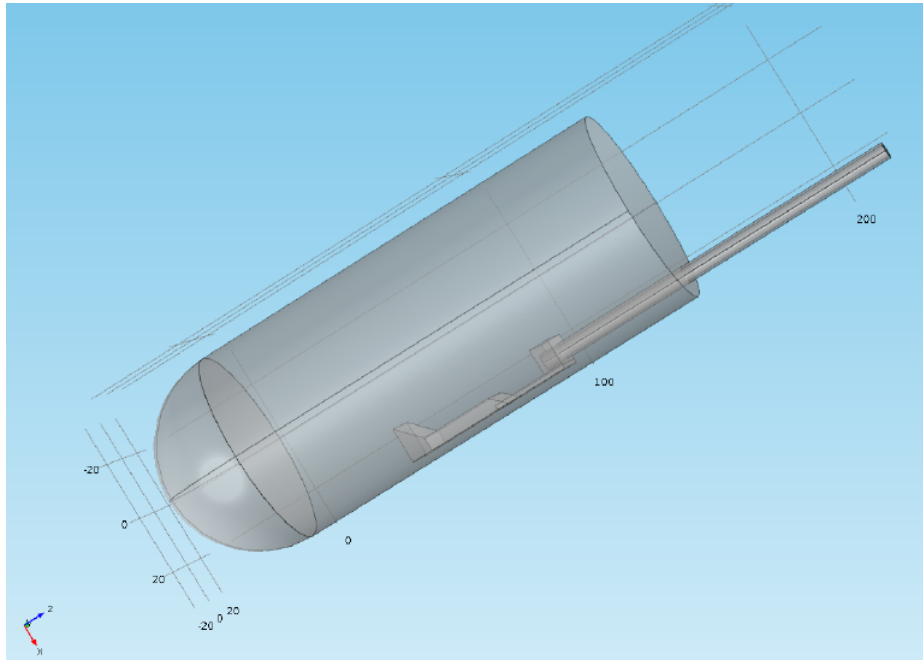


Figure 1. The benchmark nose use in the initial simulation setup. The target cells have been removed for this picture. The design was provided by JLab Target Group.

imperial information will be necessary so that the target material properties can be accurately represent to better simulate how much microwave passes though both cells at resonance. In our initial tests, different materials were tested to find one that could be used for a stand in until this information can be obtained. Mica was found to be a good approximation for a target material which still allows some (10%) microwave at 140 GHz to pass through. The absorption in the cups can be seen in Figure 2. The figure depicts a 2D slice of the simulated area around the cups. The white tube to the right is the waveguide and the thin black outline shows the two target cells. Notice that the region outside the cells indicate a complex pattern of microwaves but inside each cell is relatively homogeneous. The intensity in the image represents the electric field norm in (V/m).

3. Initial Simulations

The Microwaves were input by an open port on the end of the waveguide and the input frequency (f_0) was set to 1.4 GHz. This is an order of magnitude small than what is required but at this frequency it is possible to fully mesh and run in 3D with the hardware available. Initial simulations in 3D give a qualitative depiction of the microwave behavior in a certain cavity geometry. However for realistic quantitative analysis it is necessary to study the geometry in 2D slices so that COMSOL can handle the higher frequencies. The memory usage limitation was the major barrier for high frequency in 3D. The real experimental frequency of interest is around 140 GHz, but at this frequency the wavelength was so small that COMSOL could not make a 3D mesh small enough for a good simulation. An example of a 1.4 GHz simulation is shown in Figure 3 with the target cells switched off. This picture is a multislice of the 3D results just shows the qualitative character

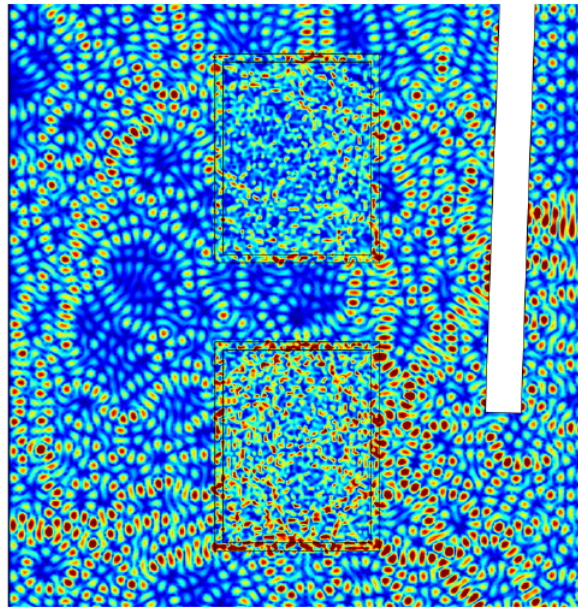


Figure 2. Close up of the simulation test cups filled with solid Mica. The white tube to the right is the waveguide and the thin black outline shows the two target cells.

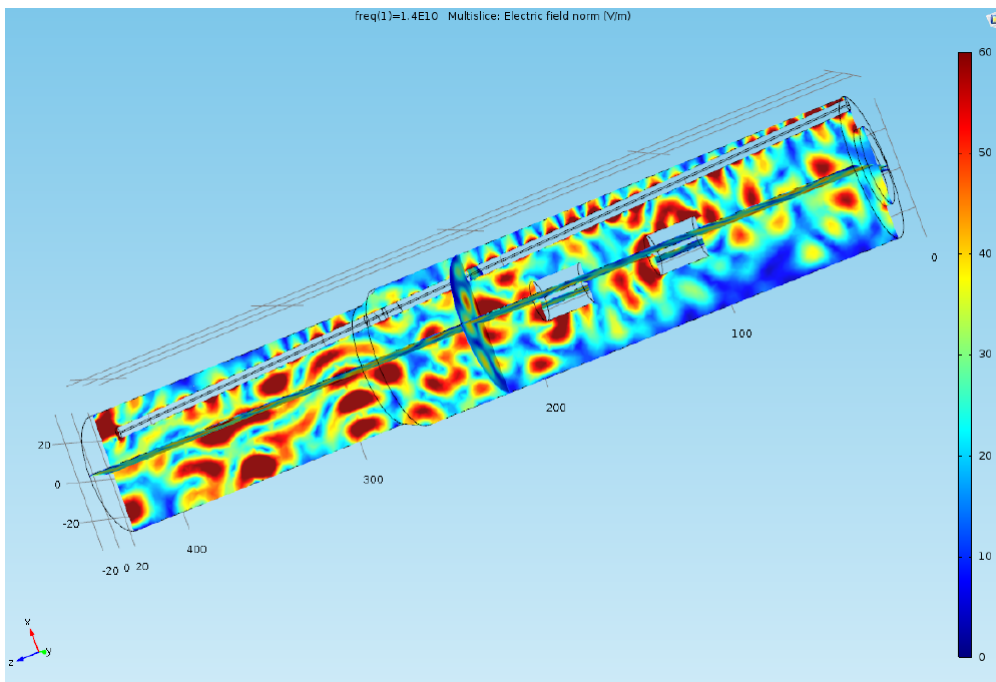


Figure 3. Example of one of the 3D simulations using 1.4 GHz. Here the target cells are switched off to show the 3D characteristics around the cells in the cryostat.

of the microwave interference pattern. The intensity in the image represents the electric field norm in (V/m).

3.1 Starting Metrics

The initial metric used to study the microwave power received at each target cell was the ratio of the surface integral of the norm of the power through each cup. The surface integral was taken over each cup individually and the ratio was calculated such that the closer to one the more even the irradiation is to both cups. The actual magnitude of the power at each cup was also an important factor. This metric is specific to the 2D simulations.

3.2 Simplified Geometry

Most of the problems that are solved with COMSOL Multiphysics are 3D in the real world. In many cases, it is sufficient to solve a 2D problem that is close to or equivalent to the real problem. Furthermore, it is good practice to start a modeling project by building one or several 2D models before going to a 3D model. This is because 2D models are easier to modify and solve much faster. Thus, modeling mistakes are much easier to find when working in 2D. Once the 2D model is verified, you are in a much better position to build a 3D model.

In this case a cross section is viewed in the xy -plane of the actual 3D geometry. The geometry is mathematically extended to infinity in both directions along the z -axis, assuming no variation along that axis. All the total flows in and out of boundaries are per unit length along the z -axis. A simplified way of looking at this is to assume that the geometry is extruded one unit length from the cross section along the z -axis. The total flow out of each boundary is then from the face created by the extruded boundary (a boundary in 2D is a line). There are usually two approaches that lead to a 2D cross-section view of a problem. The first approach is when it is known that there is no variation of the solution in one particular dimension. The second approach is when there is a problem where the influence of the finite extension in the third dimension can be neglected.

If the 3D geometry can be constructed by revolving a cross section around an axis, and if no variations in any variable occur when going around the axis of revolution, then use an axisymmetric physics interface. The spatial coordinates are called r and z , where r is the radius. The flow at the boundaries is given per unit length along the third dimension. Because this dimension is a revolution all flows must be multiplied with αr , where α is the revolution angle.

To simulate the frequency of interest we compromise the model by creating a 2D representation of a middle slice. An arbitrary number of slices can be studied in 2D to get a limited picture of the microwave behavior in a 3D structure. By decreasing the total number of mesh elements so considerably it is possible to study the frequency range of interest. This does require a fictitious dimension out of the page to be extended forever in order to construct the boundary. Exploring this option we focus on a single slice of the full cavity along the center of the waveguide. The simplification and boundary condition makes it difficult to model accurately, but we first just try to explore this option's viability.

Figures 4 and 5 show the variability of the 2D simulation process, and how much control over the geometry of the slice this method gives the user. Figure 5 in particular is representative of how much the cavity geometry affects the way the microwaves propagate throughout the space. The picture shows the 2D simulation results using two Mica filled cups with a vertical slice down a hypothetical nose cavity. The waveguide is seen in white with the two Mica target cells outlined in

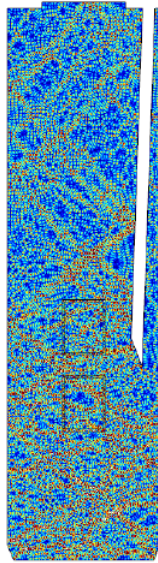


Figure 4. The initial 2D simulation using two Mica filled cups for a vertical slice of the nose cavity. The waveguide is seen in white with the two Mica target cells outlined in black.

black. This study shows the variation in the microwave distribution resulting from moving the tip of the cavity changing the reflections in the geometry.

We then build models based on the *modern* JLab nose design show in Figure 6. This design contains a positioned wave guide, a plastic bath tube for liquid helium, the target cells and the more realistic aluminum nose piece. In the figure show to the right is our 2D slice using all the same materials except for using whole Mica cell rather than Kel-F and NH_3 . It is clear from the picture that in this crude approximation the empty nose space receives the majority of microwaves. The bottom cell is closer to the region and receives more microwave power.

Figures 7 show variations in the geometry of Figure 6. Three other variation of the bottom of the nose cavity are shown. Though we show only the qualitative results here its clear that the sharp concave geometry to the left has greater microwaves that move up towards the cups. A visible intensity region is show moving upward. This is due to the reflection of the sharp angle at the bottom. Its not clear why the other two show such even but low intensity throughout.

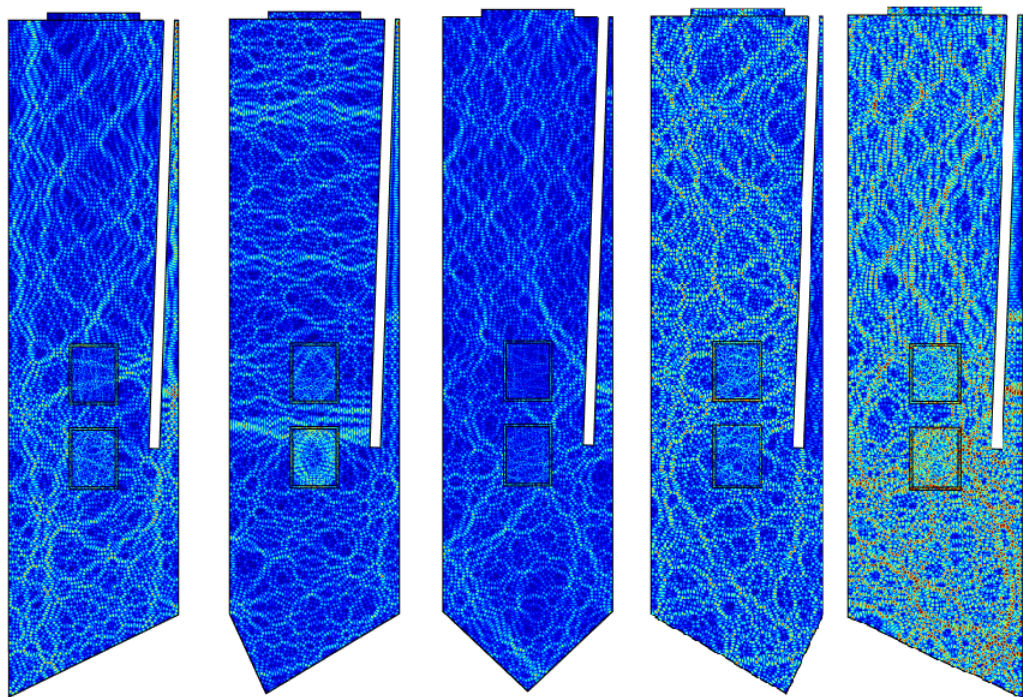


Figure 5. The 2D simulation results using two Mica filled cups for a vertical slice of the nose cavity. The waveguide is seen in white with the two Mica target cells outlined in black. This study shows the variation in the microwave distribution resulting from moving the tip of the cavity changing the reflections in the geometry.

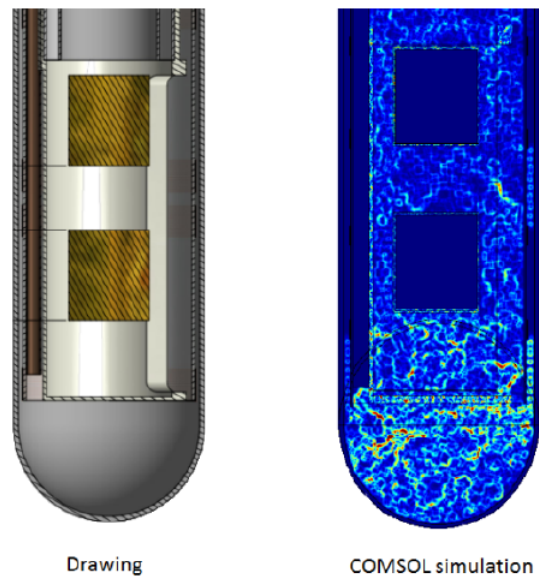


Figure 6. The Jlab *modern* nose design (on the left) which contains a positioned waveguide shown as the dark tube on the left of the cavity, a plastic bath tube for liquid helium shown in white, the target cells show in light brown and a realistic aluminum nose piece. In the figure show to the right is our 2D slice using all the same materials with the same dimensions except we used whole Mica cells rather than Kel-F and NH_3 . The waveguide is dark in the same position with the two Mica target also dark.

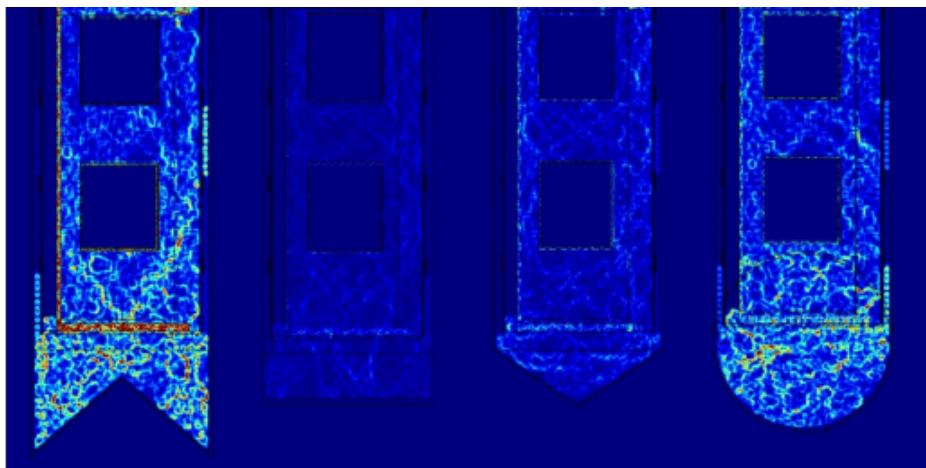


Figure 7. The 2D simulation results for Mica filled cups. This picture represents a vertical slice down a hypothetical nose cavity. Here we should the results of four different possible nose ends and the resulting microwave relative intensity of the electric field norm.

3.3 Further Limitations

The RF Module has a dedicated period condition. The periodic condition can identify simple mappings on plane source and destination boundaries of equal shape. The destination can also be rotated with respect to the source. There are three types of periodic conditions available. The first is Continuity which is the tangential components of the solution variables are equal on the source and destination. There is also Antiperiodicity which means the tangential components have opposite signs. Then there is Floquet periodicity which means there is a phase shift between the tangential components. The phase shift is determined by a wave vector and the distance between the source and destination. Floquet periodicity is typically used for models involving plane waves interacting with periodic structures. Periodic boundary conditions must have compatible meshes.

Electromagnetic radiation propagates freely as a traveling wave in the absence of boundary conditions. In perspective of the Helmholtz Equation, Sommerfeld wrote the condition of radiation as

$$\lim_{r \rightarrow \infty} r \left(\frac{\partial u}{\partial r} - iku \right) = 0 \quad (3.1)$$

which demands that energy completely vanishes at infinity. This condition is necessary for simulating infinite free space. Since COMSOL simulations must always have boundaries, free space must be approximated beyond the domain. The Scattering Boundary Condition function uses

$$\mathbf{n} \times (\nabla \times \mathbf{E}) - ik\mathbf{n} \times (\mathbf{E} \times \mathbf{n}) = 0, \quad (3.2)$$

an incarnation of the Sommerfeld condition. By applying the Scattering Boundary Condition to the boundaries of the simulated domain, continuity can be maintained past the boundaries. Figure 8 shows a one dimensional slice of a system with and without SBC.

Free space is important to establish in these simulations so as to show the behavior of radiation in the absence of boundary conditions. Section 4.2 shows that systems at 140 GHz are extremely sensitive to small geometric changes ($\approx \lambda$) and can make it difficult to understand the general behavior of the microwaves. It's therefore important to see how changes to the geometry of the system can affect target irradiation independently of resonance.

The other issue with the limits of our simulations is how the necessary free space to properly setup the boundary condition technically represents the wrong geometry. For all of the 2D simulation so far generated the dimension into and out of the page is infinite which at best can only provide a crude approximation of what we are interested in by using a long rectangular-like geometry where we take a vertical slice for our analysis. For open geometries this provides a reasonable test ground to explore both qualitative behavior and making some quantitative comparisons.

4. Empirical Studies

4.1 Material Studies

As mentioned we only approximated the target material using the COSMOL preset material Mica to use as target material. To improve the representation of the target material we measured the

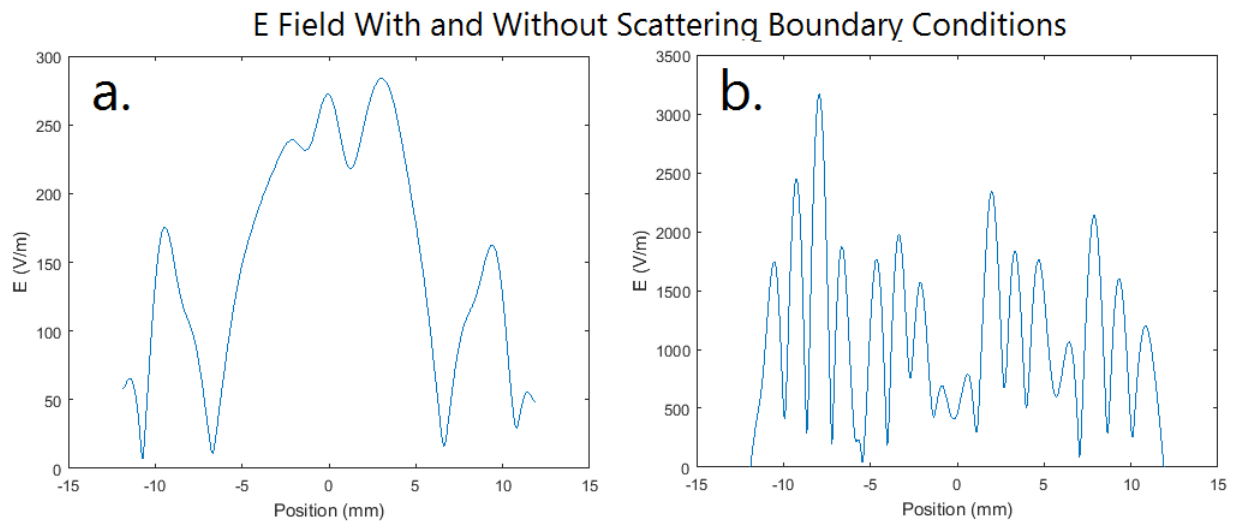


Figure 8. The E field along an arbitrary slice of the domain. a) In the presence of Scattering Boundary Conditions, the E field is nonzero at the boundary. b) In the absence of Scattering Boundary Conditions the E field vanishes at the boundary.

degree of absorption of NH_3 beads at resonance in a DNP system. The bulk properties of the preset materials in COMSOL are usually very generic and have to be studied in detail to be more realistic. Figure 9 shows how one can add different layers to construct a particular absorption and attenuation behavior. Bulk properties such as relative permeability, relative permittivity, electrical conductivity, and density are used to characterize the materials used in COMSOL. These values can be tuned to get to absorption matching to what we measure in experiments. The microwave absorption properties of a material have a particular dependence on relative permittivity and relative permeability of the medium. We insert known the parameters on solid ammonia and then match to our experimental results.

The DNP test setup is standard except that we try to constrain the direction of the microwaves used by creating a foil cylinder around the horn and target cell. The foil is sealed to the horn rim with cryogenic glue. This is also done around the target cell so that the microwaves have only the direction of the target cell to pass through. This significantly reduces the amount of irradiation at the target cell from indirect microwaves that are bounding around in the cryostat. Our sensor configuration consisted of one sensor about 1" above the target cell and the other one 1" below. The sensors use were Vishay RCWP-575 $1\text{K}\Omega$ with a tolerance of 1%. We then did a baseline study to measure the change in resistance by reducing the power to the cryostat by increasing the attenuation and measuring the change in resistance in comparison to the liquid helium boil off from the microwaves. In this way we calibrate the Vishay sensor to measure the degree of power change.

We then take data with microwaves on from the two sensors with and without material in the target cell. The top sensor saw no measurable change while the bottom sensor indicated a drop in microwave power of about 20%. We repeated the measurement a few times to see similar results. The packing fraction we measured for this particular target load was 62%. This is measured by breaking down the material after the measurement. The NH_3 is compressed in to minuscule grains

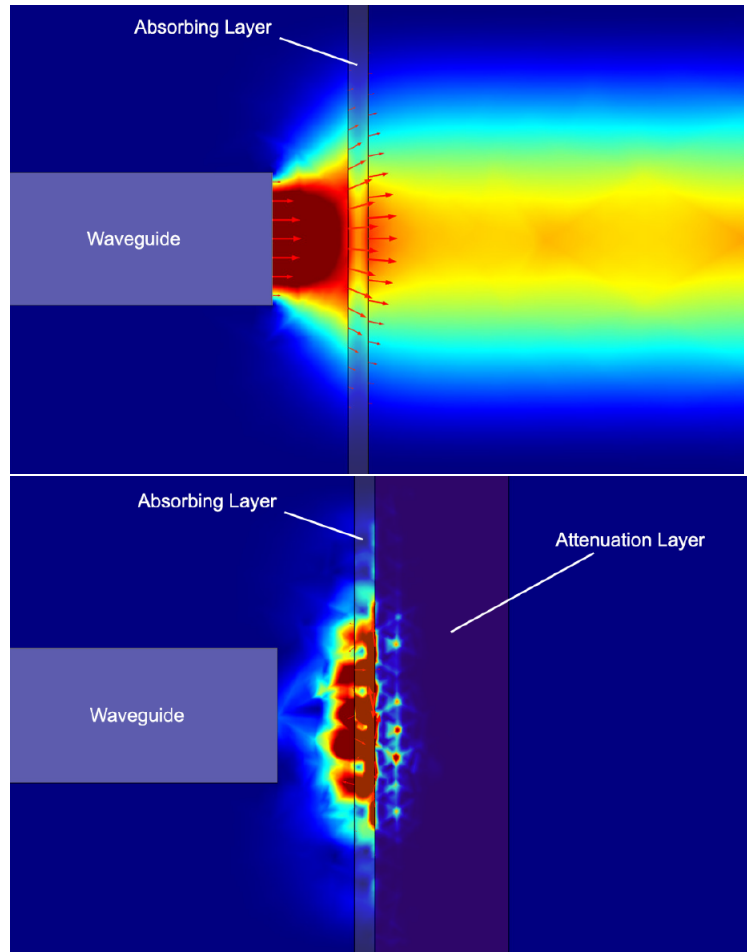


Figure 9. The top picture show COMSOL simulations with a think microwave absorbing layer. To construct a barrier to stop microwaves an attenuation layer is added.

(slush) and then the volume is measured while pressing the LN₂ out of the space.

The simulation of the cryostat was 2D with a foil region again connecting the horn and cup but in this case we use an open geometry so instead of the cavity it just a tube with microwaves passing in one way. This is the most realistic setup for studying with the 2D method. In this way its possible to represent the most defining feature of the test without unintentionally setup artificial resonance patterns. So even though the outer cavity is rectangular and infinite in two directions rather than the real cylindrical shape the microwaves are passing right through so we can study smaller local dynamics. So part of the tools to make COMSOL represent a realistic sandbox is to have the outer open but also large with respect to the scale of interest.

The relative permeability and relative permittivity were then varied in COMSOL so that the same volume of ammonia also reduces the power that passes through be 20%. Figure 10 demonstrates the propagation of microwaves through two different styles of target cells. The cup (perimeter) is Kel-F which is a modified version of the COMSOL preset for plastic. COMSOL was then able to predict with in about a 1% accurate the power reduction when we put two target cells at resonance in the microwave pass. It is worth noting that experimentally we find no difference in

Property	NH ₃
Relative Permeability	6
Electrical Conductivity	2.01×10^{-15} S/m
Relative Permittivity	4.95
Density	0.917 g/cm ³
Heat Capacity	8.8×10^{-6} J/(Kg K)
Thermal Conductivity	2.3×10^{-3} W/(m K)
Refractive Index (real)	2.45
Refractive Index (Imag)	0

Table 1. Characteristics of solid ammonia used in the COMSOL simulations.

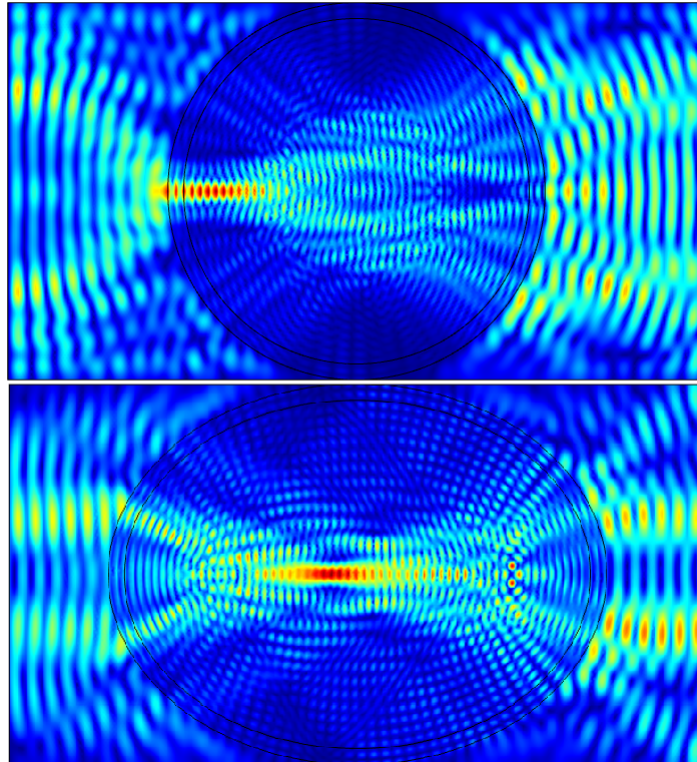


Figure 10. Interaction of electromagnetic radiation inside solid ammonia in the COMSOL simulation. Linearly polarized radiation enters the domain from the right and travels to the left. The top picture depicts a circular cup while the bottom depicts an elliptical cup.

the heat load at the bottom sensor when the ammonia is not at resonance and the microwaves pass right through.

4.2 Microwave Cavity Studies

Figure 11 illustrates the weak interactivity between low frequency (10 GHz) radiation and new more realistic version of NH₃ targets in a 3D system. We return to the original prototype from Jlab. Though this is the wrong frequency this is likely a decent representation of the spatial distribution of microwaves in the target cells held in a cylindrical partial closed cavity.

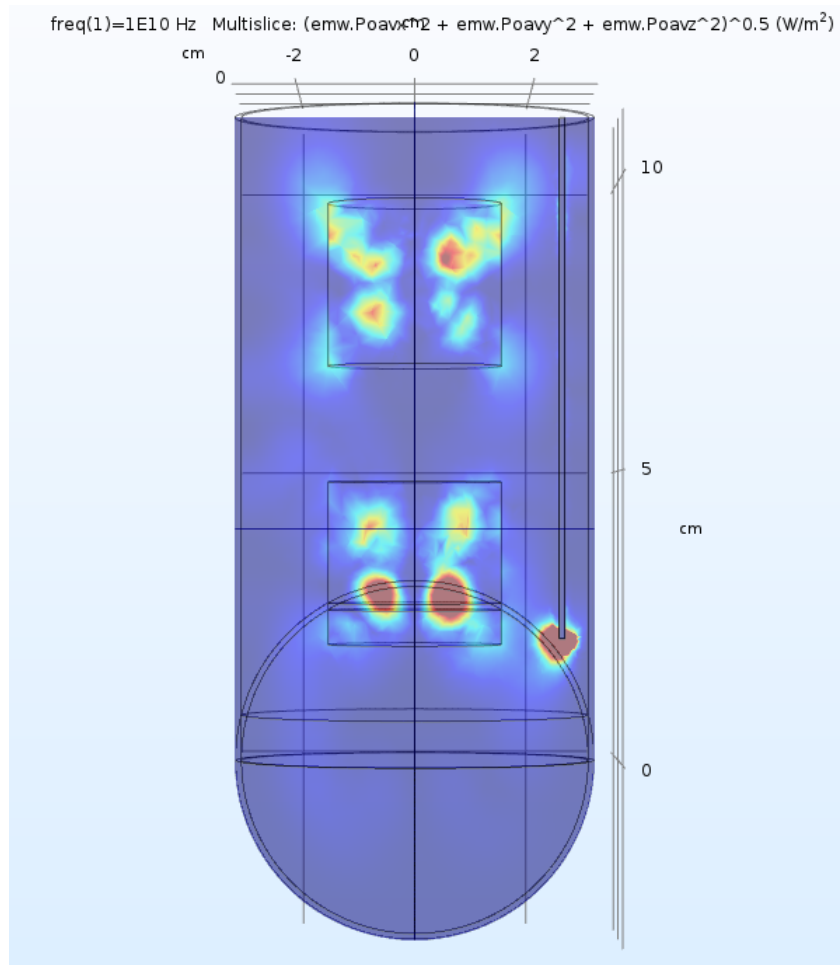


Figure 11. Microwave distribution in a 3D cavity at 10 GHz. Irradiance in the targets is unevenly distributed and there appear to be only weak wave solutions in the empty space.

In traveling wave solutions, the orthogonality condition between the E field, B field, and direction of propagation require three spatial dimensions. Even in COMSOL's 2D Cartesian model, the geometry is extruded into the z direction by a unit vector so that Maxwell's equations are satisfied.

Studies on the effective "wafer" geometry of the 2D simulation module helped in understanding a few important properties of light. The excitation modes in a cavity arise from the requirement that $E_{||}$ have 0 amplitude at the boundary of a reflector. Figure 12 shows the sensitivity of the modes due to this condition. Variation of the geometry by 1 mm ($\frac{\lambda}{2}$) drastically changed the distribution of microwaves in nearly identical cavities, this is especially true for closed or semi-closed geometries.

4.3 2D Axisymmetry and Microwave Heating

Though for some situation the 2D Cartesian models at proper frequency and the 3D models at lower frequency can provide some insight neither offer a comprehensive picture of microwave distributions for cylindrical geometries. The COMSOL 2D Axisymmetric modeling adds some additional information that can be useful. Also included in COMSOL is a microwave heating module that

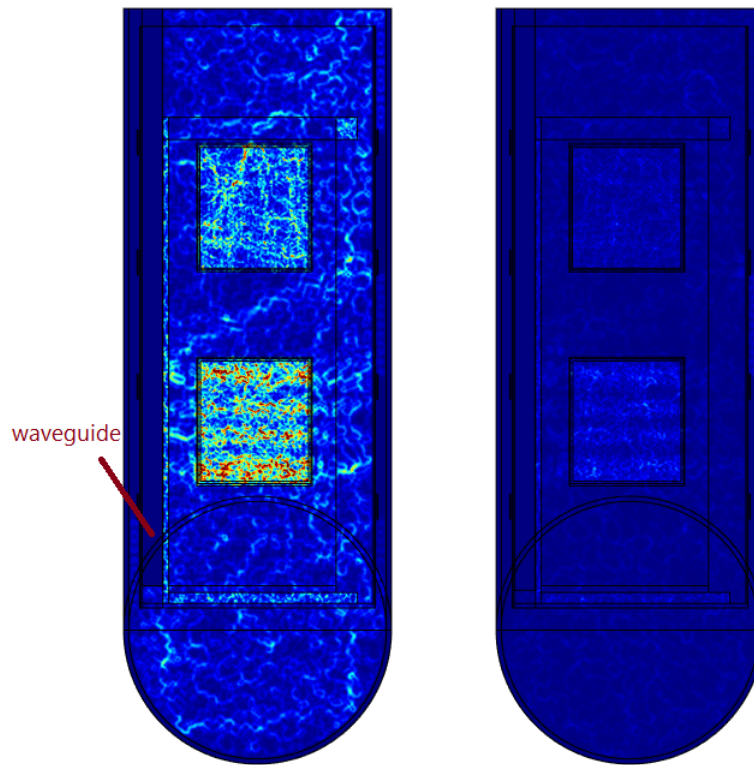


Figure 12. Microwave distribution in nearly identical asymmetric 2D Cartesian cavities. The cavity on the right has had its waveguide shifted down by 1 mm. The contrast in target absorption highlights the sensitivity of excitation modes in a large geometry.

allows the user to simulate the thermal effects of microwaves interaction with matter. As a means of testing the effectiveness of 2D axial symmetry studies in simulating energy distributions, an aluminum cavity was constructed in the lab.

As a qualitative check we used thermochromic liquid crystals film and placed it in a cylindrical nose piece. The same exact geometry was constructed in COMSOL. After microwave irradiation we pull the film out and photographed the pattern so compare to the COMSOL simulated results. Though its not particularly visible in the photo there is similar structure and patterns seen from the simulation seen in Figure ???. The film changes temperature quickly so the fine structure drops away pretty fast.

A silica glass rod was hung from the standard conical gold plated horn to locate our sensors. Two thermistors were then attached to the rod to detect temperature changes in the cavity.

The metric used to determine the effectiveness of the microwave heating simulation was the ratio of temperatures of the thermistors. This ratio is conceivably the same as the ratio of microwave power absorbed by each thermistor. We first conducted a careful selection procedure for the thermistors to ensure similar characteristics over the same temperature range of interest. These studies are performed in open air at room temperature and no cryogenics.

Figure 14 shows the thermistor ratio over the course of 60 seconds beginning at time 0. The

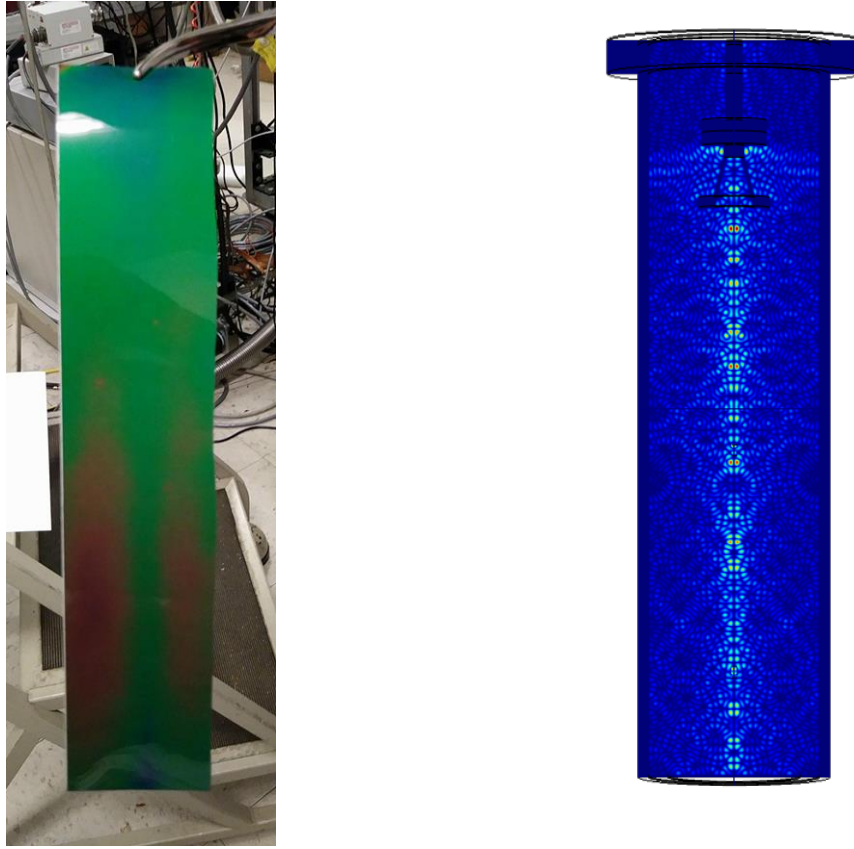


Figure 13. Comparison of thermochromic liquid crystal film and COMSOL simulation using the 2D axisymmetric configuration of a cylindrical open ended cavity.

constant error of 0.0034 in the experimental ratio ensures that every data point falls within one σ of the COMSOL data. However, at the end of the time period, the two curves begin to diverge. Thermistors are made of metallic oxides, pressed into a small cylindrical shape and then encapsulated with an impermeable material such as epoxy or glass. We try to construct a similar composition in our model but to accurately represent these types of units would take a study of its own. It is clear enough that doing so is possible. The resulting plot of the test cavity at near the beginning of the test and near the end is shown in Figure 15. The heat plot here is showing the temperature in Kelvin.

The 2D axisymmetric model provides promising data on the temperature ratios in the absence of comprehensive material information. There were also a number of small physical inconsistencies with the experimental setup, such as imperfections with the axisymmetry and exact positioning of the sensors. These results do indicate a very promising option for studying systems that can be represented with the axisymmetry option.

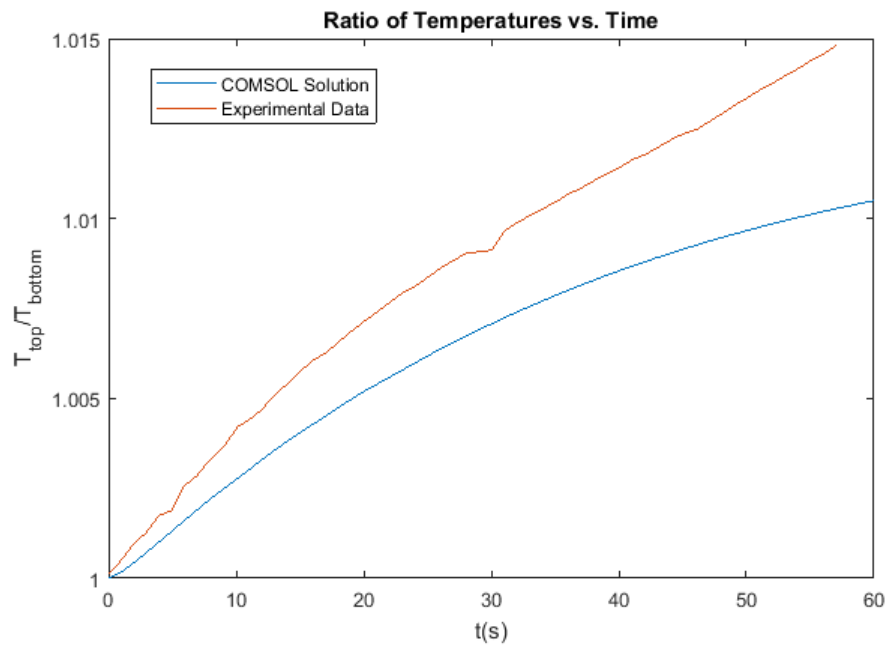


Figure 14. Temperature ratio between the top and bottom thermistors as a function of time.

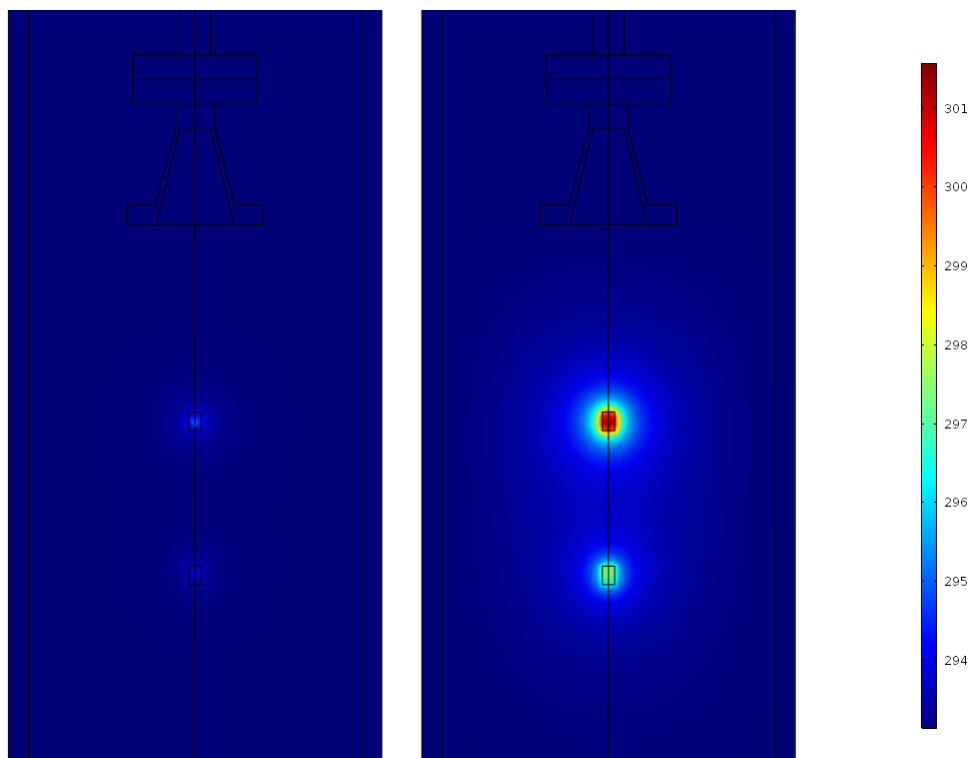


Figure 15. COMSOL simulation results showing the heat plot of the test cavity at 5 s (left) vs. 60 s (right). The heat plot here is showing the temperature in Kelvin.

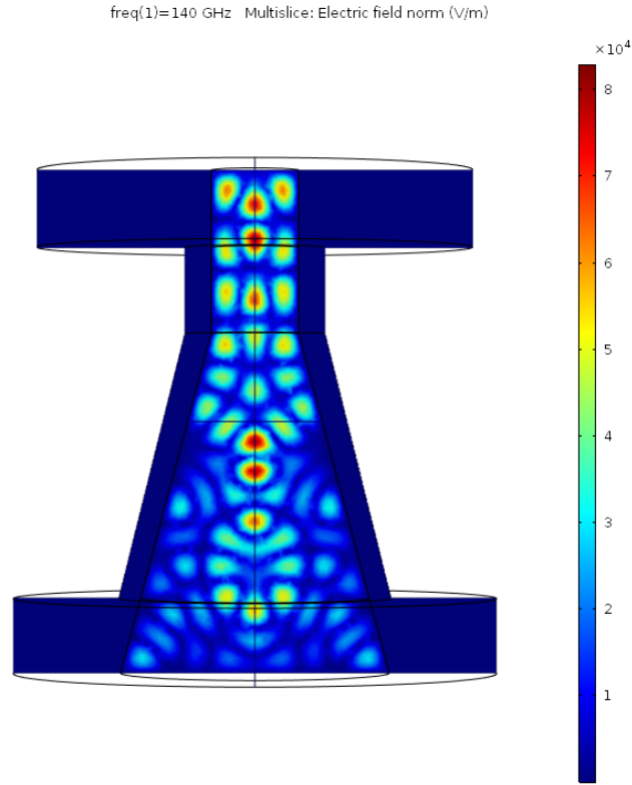


Figure 16. Simulation of the standard conical gold plated microwave horn showing 3D simulation at 140 GHz. This picture is showing 3D multislice of the electric field norm (V/m).

4.4 Horn Studies

There are many aspects of the microwave system that can be simulated directly with COMSOL even for small wavelengths assuming that the geometry of interest is not much bigger than the wavelength of interest. Waveguides and the microwave horns are good examples of this, see Figure 16.

The dispersion from the waveguide upon delivery to the target cell can be managed with a microwave horn attachment at the mouth of the waveguide. Some interesting questions came up in previous cooldowns around the possibility of a power dependence seen in the distribution of the microwave. It is well known that the EIO generator has power variations that depend on cathode voltage and frequency. There may also be a change in power due to dispersion, cavity geometry, reflection and absorption from different resonant modes that are also sensitive to frequency changes. This becomes a concern when trying to irradiate a long target cell uniformly or two separate target cells equally.

To look at this a bit closer we used a gold-plated horn attachment to irradiate three target cells (Figure 17). Due to the size of the horn, 3D simulations were not possible, but its Cartesian geometry allowed for division into 2D XZ and YZ domains.

Figure 18 shows wave propagation from the horn in the XZ (a) and YZ (b) domains. The boundaries of the geometry have been coupled with Scattering Boundary Conditions so as to get

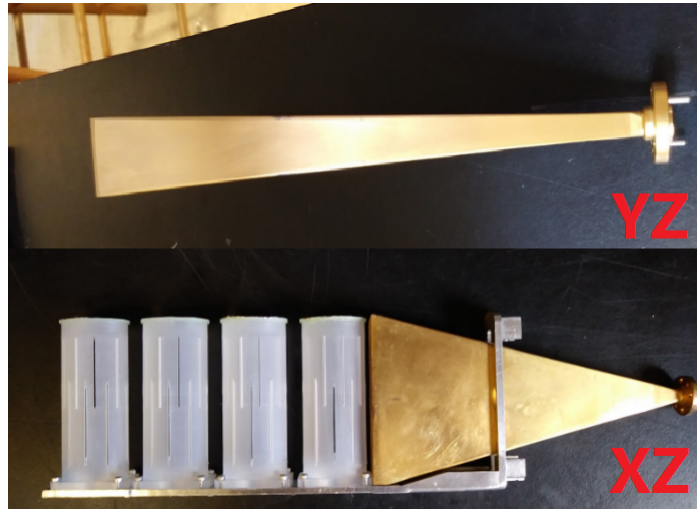


Figure 17. Photographs of the gold-plated horn. The cup configuration of the XZ picture is not the configuration used for the simulations or the Spring 2018 Cooldown experiments.

traveling wave solutions. As one might expect, the furthest two cups see significantly less microwave irradiation than the closest (Figure 20) Normally this is not an issue due to the microwave bouncing around in the nose. However to set up a configuration that we can match in simulation to study frequency dependence we again use foil to limit the domain of the microwave in the real empirical test. We also use three Vishay chip resistors on each of the 8 cm long target cells equally spaced apart. Adding reflecting geometries to the cavity can increase target absorption under certain circumstances. Surrounding the targets with reflecting walls will decrease free propagation and make the system more sensitive to resonance conditions. We also add into the COMSOL simulations the aluminum target ladder and Kel-F cups. For this test with leave the cups empty. Figure 21 shows the COMSOL results of this construct.

For the empirical study data was collected during the cooldown at 1 K to increase the sensitivity to the microwave power distribution measurements. Once the temperature was stabilized the microwave was turned on and left on at a particular frequency. The frequency was change from 140.0 GHz to 140.6 in four steps with several seconds at each step and then back to 140.0 in the same frequency and time steps. The change in sensors from this study can be seen in Figure 23. The plot looks somewhat symmetric about the central time line because the frequency dependence exhibited some degree of reproducibility. So going back to a particular frequency would reproduce the same power distribution received by the set of sensors. Some of this is thought to be from resonance patters and some is thought be caused by diffraction patterns. The COMSOL results to this study are shown in Figure 22. There is clearly a spatial response to the microwave power profile which changes with frequency.

Mock chip resistors where added to the simulations making obstructions inside the geometry and seem to indicate significant wave diffraction patterns. Figure 24 shows the diffraction of incident radiation and the resultant direction of propagation.

In the COMSOL simulation the total time-averaged power reaching all of the cups was measured with and without the presence of thermistor chips. The respective 0.0599 W and 0.0637

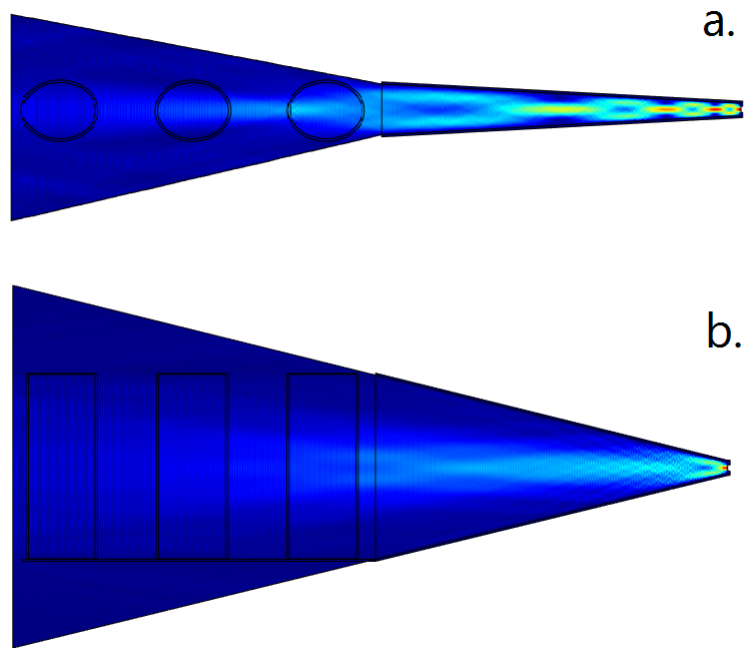


Figure 18. COMSOL image of the XZ and YZ domains. Radiation is emitted from the right and reaches the target cups.

Measurements showed that the resistor chips decrease the absorbed power by 6.3%. From the image, it also appears to redirect the microwaves.

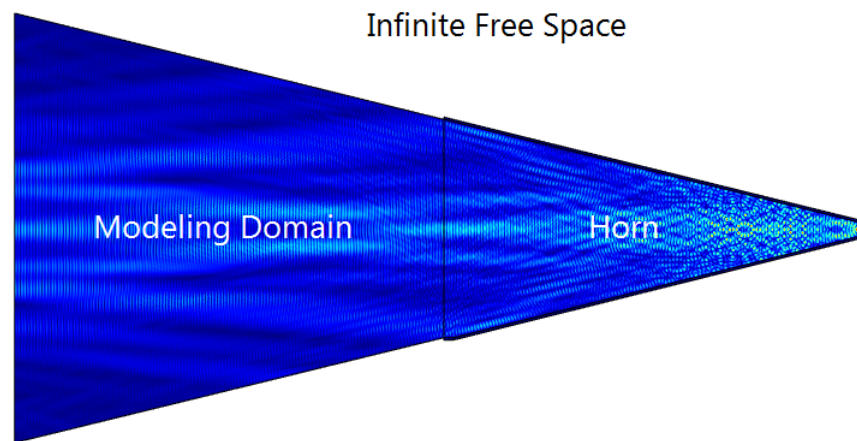


Figure 19. Infinite Free Space.

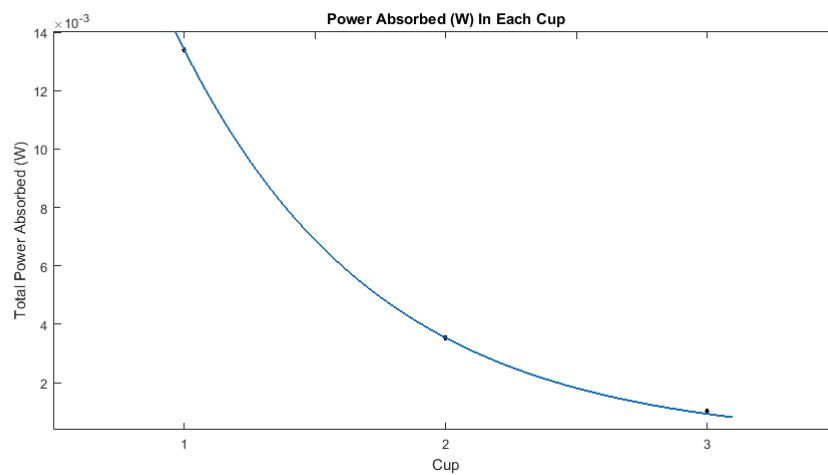


Figure 20. Electromagnetic power reaching each target in the line of the microwave path.

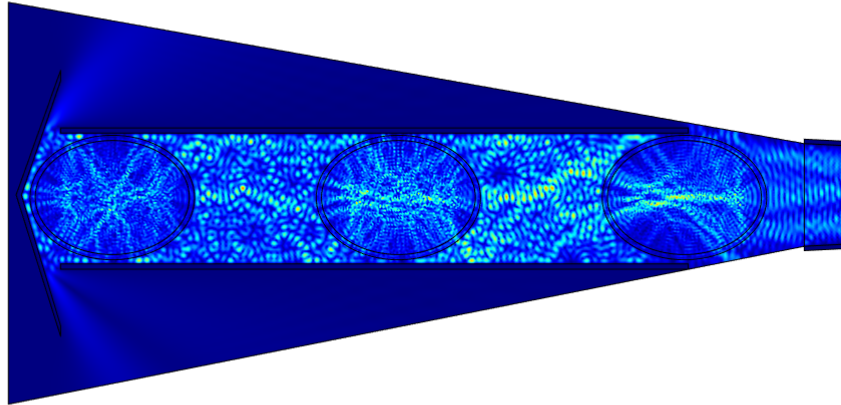


Figure 21. Simulation of the described geometry showing the ladder and inside the target cells.

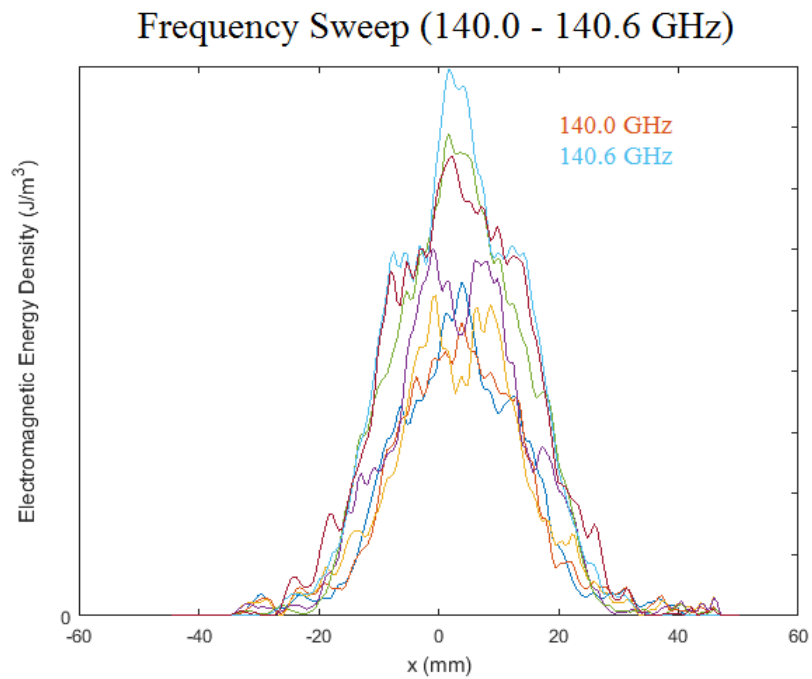


Figure 22. The COMSOL results for the described geometry over a frequency range from 140.0 GHz to 140.6 GHz using 0.1 GHz steps. Showing a spatial response to the frequency changes.

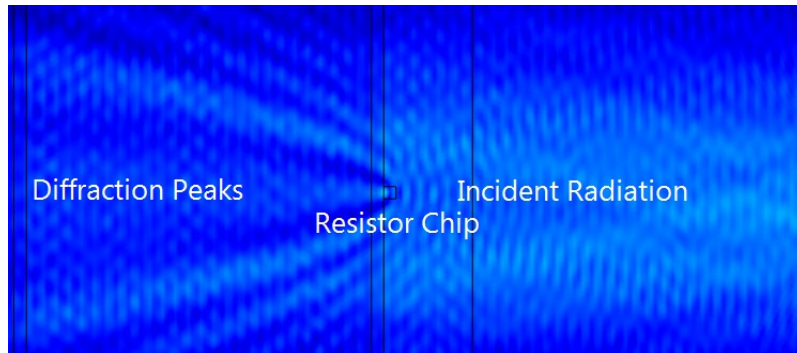


Figure 23. The empirical sensor data showing the change in resistance (heat from microwave) from 140 GHz to 140.6 GHz in four steps and then back. Red and brown are two sensors on the top cup and blue and orange are two sensors in the same relative position but on the bottom cup.

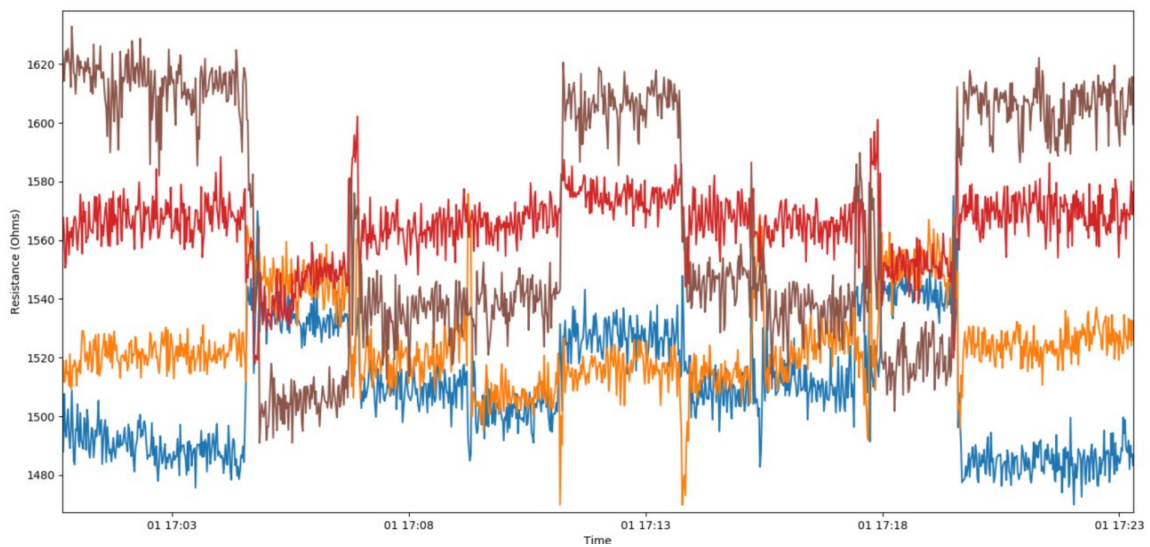


Figure 24. Microwave diffraction due to a resistor chip.

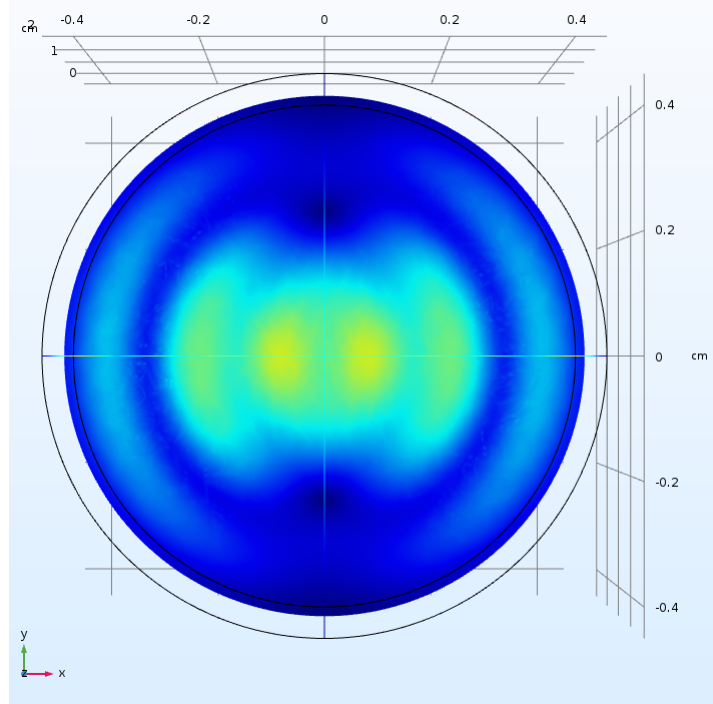


Figure 25. Transverse solution of the E field in a circular waveguide. There is no radial symmetry due to the linear polarization of the radiation.

5. Waveguide Studies

The efficiency of guided-wave geometries is crucial in transporting microwaves from the EIO generator to the reflecting cavity. While sample may have some small range of frequency dependence, the intensity of an incident beam and evenness of target irradiation ensure that more nuclei per cell are polarized.

Boundary conditions for the interaction of E and B fields at the surface of a conductor create equations of motion in the form of Bessel's equation [1].

$$\left[\frac{\partial^2}{\partial x^2} + \frac{\partial^2}{\partial y^2} + \left(\frac{\omega}{c}\right)^2 - k^2 \right] E_z = 0 \quad (5.1)$$

$$\left[\frac{\partial^2}{\partial x^2} + \frac{\partial^2}{\partial y^2} + \left(\frac{\omega}{c}\right)^2 - k^2 \right] B_z = 0 \quad (5.2)$$

Wave solutions for electromagnetic radiation propagating through circular waveguides are separated into three components (the solution is not dependent on angle θ due to radial symmetry.).

$$\Psi_n = R_n(r)Z(z)T(t) \quad (5.3)$$

The radial component to the solution is also a solution to Bessel's equation. This fact provides a sanity check for simulations, meaning that for systems of high energy transfer, the transverse image of the solution should be a Bessel function.

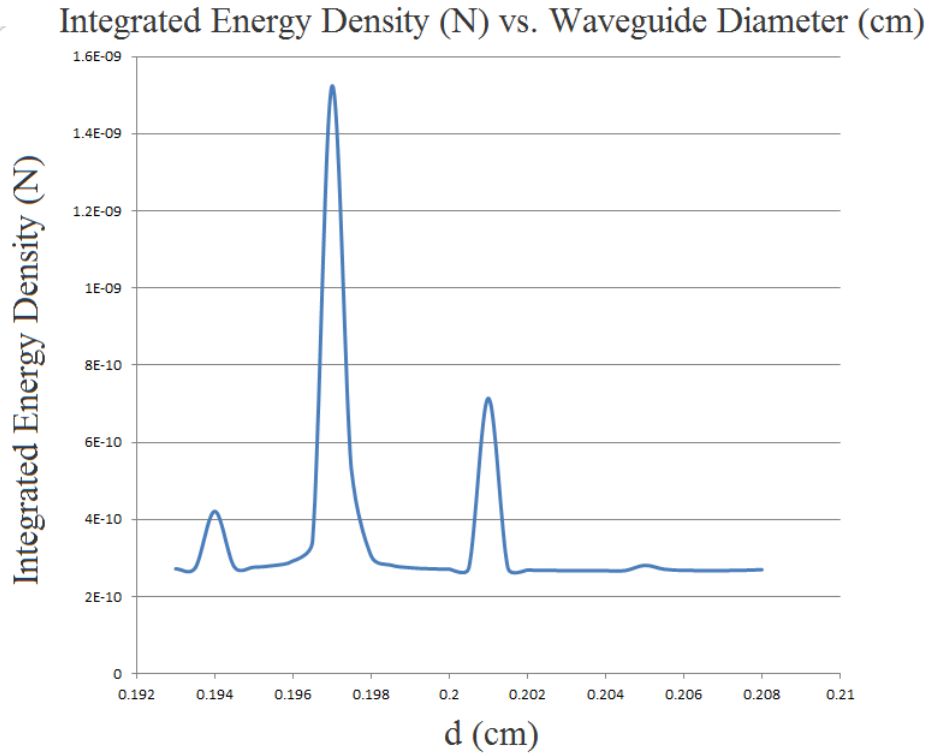


Figure 26. Integrated Electromagnetic Energy Density with variations in the waveguide diameter. Resonant peaks correspond with Bessel functions.

Circular waveguides used to deliver microwaves at 140 GHz generally have a diameter of 2 mm. To determine how sensitive the wave solutions are to variations in the diameter, the diameter of a circular waveguide was swept around 2 mm. The metric used to derive effectiveness of energy transfer was the electromagnetic energy density integrated over the output of the waveguide.

$$\oiint \frac{1}{2} \left(\epsilon_0 E^2 + \frac{1}{\mu_0} B^2 \right) dA \quad (5.4)$$

Variations around the 2 mm radius at 0.005 mm increments showed a smooth linear background with several sharp resonant peaks. Figure 26 shows two important results. The first is that in the background there is no Bessel function that matches the boundary conditions of the waveguide. At each resonant peak, there is a Bessel function that goes to zero at the boundary, therefore creating a full solution to the wave equation with Dirichlet conditions.

The second result is that the resonant peaks are very sharp and have widths on the order of 10^{-5} m. This would make it very difficult for a lab to machine a waveguide so that it's geometrically configured for resonance. It would be much easier to vary the frequency of propagating microwaves. Converting the peak widths into frequency space shows that each peak has a bandwidth of 15 MHz. If a lab has a wave generator capable of changing frequency on that order, a waveguide could conceivably be tuned for resonance.

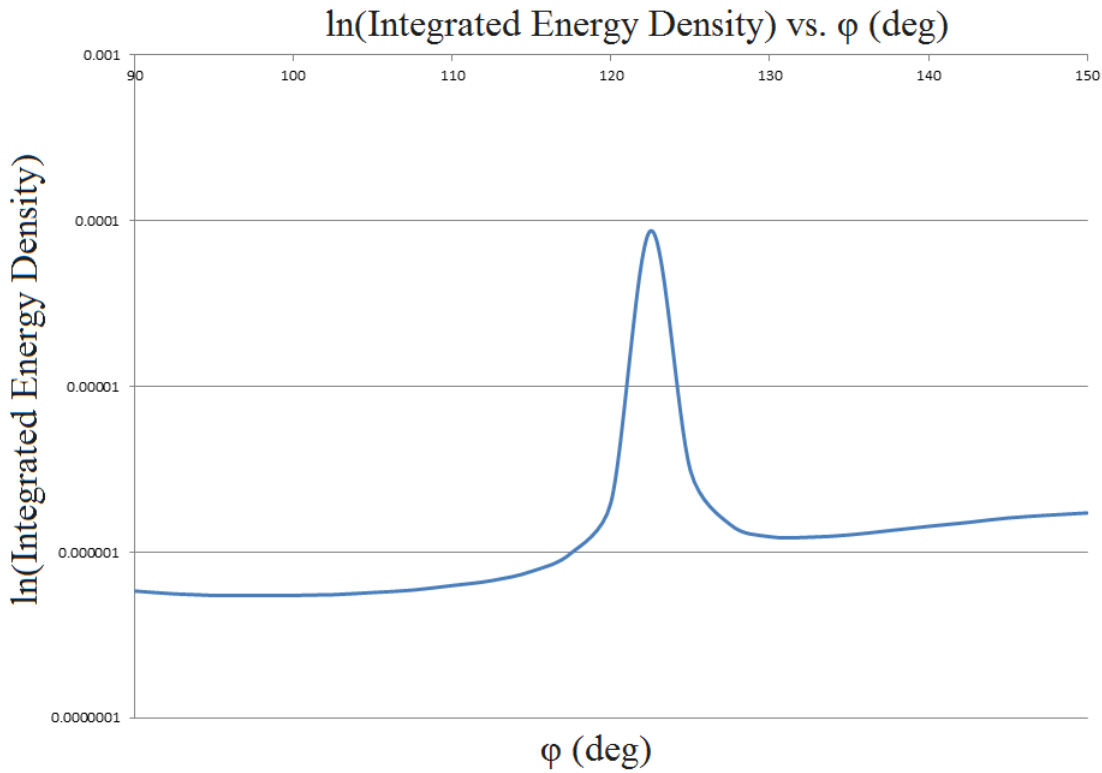


Figure 27. Logarithm of the energy density integrated over the surface of the four slots as a function of slot angle.

5.1 Slotted Waveguide

A slotted waveguide can be used as a means of controlling the dispersion of microwaves. Rather than having light disperse longitudinally along the length of the cavity, photons can escape through slots situated close to targets for more effective irradiation.

A series of studies were conducted on a closed circular waveguide with four slots. Each slot was rectangular and had a z length of $\lambda = 2.1414$ mm. Variations in the slot arclength $r\phi$ (Figure 29) showed a sharp resonant peak around $\frac{\lambda}{\phi}$. Figure 27 shows that the amplitude of the resonant peak is so intense that the vertical axis had to be adjusted to a logarithmic scale. Changing the slit spacing d from $\frac{\lambda}{2}$ to λ maintained this result.

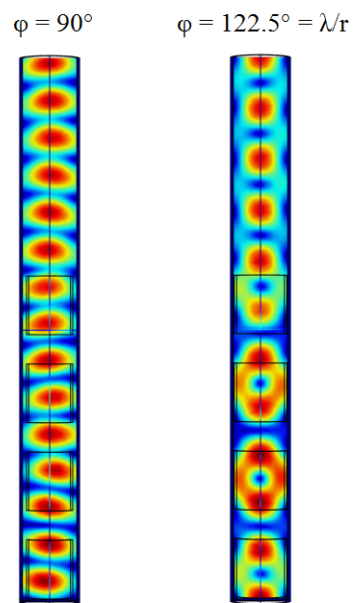


Figure 28. Longitudinal wave solutions in a slotted circular waveguide with a slot angle of 90° vs. 122.5° ($\frac{\lambda}{r}$). Color maps in this figure are not equally scaled. The power being transferred through the slots in the right waveguide is several order of magnitude larger than in the left.

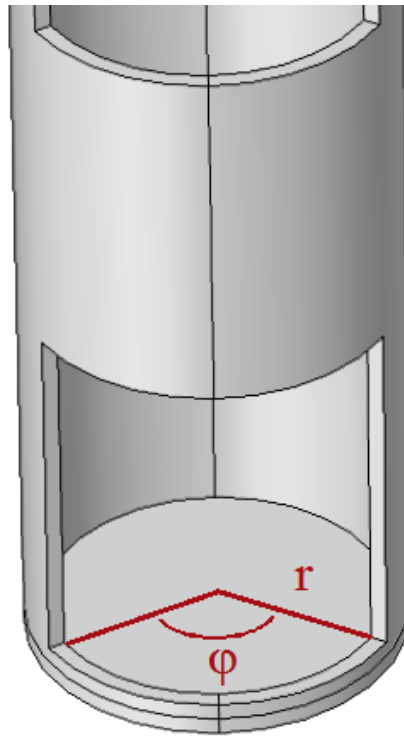


Figure 29. Closed slotted waveguide.

6. Conclusion

COMSOL Multiphysics 5.3 can be used to simulate various microwave conditions to better understand how to optimize transfer and geometry at various design and prototyping stages. These studies are meant to study both the less understood behavior of microwaves in a cryostat but also the validity of the COMSOL suite for this particular application.

There are some interesting results that should be investigated further but at this stage it is safe to conclude that COMSOL is very helpful for a limited number of real world testing scenarios with DNP microwaves. We hope these studies are useful as a starting point to more in depth look in the near future.

References

- [1] Comsol RF User Guide Version 4.3 May 2012, 1998–2012 COMSOL
- [2] Sommerfeld, A., Straus, E. G. (1949). *Partial Differential Equations in Physics*. New York: Academic Press.
- [3] Griffiths, D. J. (2017). *Introduction to electrodynamics*. Cambridge (Reino Unido): Cambridge University Press.
- [4] Alvarez, A. F., Franco-Mejia, E., Pinedo-Jaramillo, C. R. (2012). Study and Analysis of Magnetic Field Homogeneity of Square and Circular Helmholtz Coil Pairs: A Taylor Series Approximation. 2012 VI Andean Region International Conference. doi:10.1109/andescon.2012.27
- [5] D. G. Crabb and W. Meyer. Solid polarized targets for nuclear and particle physics experiments. *Annual Review of Nuclear and Particle Science*, 47(1):67– 109, 1997.